

Effect of tractive force using a temporary screw type anchorage device in alveolar bone – Stress analysis using the three-dimensional finite element method –

Akihiro Nakajima¹, Masahiro Nakajima^{2,3}, Yuichi Shoji² and Kenji Kakudo²

¹Graduate School of Dentistry (Second Department of Oral and Maxillofacial Surgery), and ²Second Department of Oral and Maxillofacial Surgery, Osaka Dental University, and ³Department of Dentistry for Disability and Oral Health, Osaka Dental University Hospital, 8-1 Kuzuha hanazono-cho, Hirakata-shi, Osaka 573-1121, Japan

We used the three-dimensional finite element method to construct a three-dimensional model of the maxilla to evaluate the utility of the temporary anchorage device (TAD), and to investigate stress changes affecting the alveolar bone after the extraction of the first premolar. An outline of the model was fabricated from CT image data with the contours following extraction using the stress analysis software Mechanical Finder version 6.2 (Research Center of Computational Mechanics, Tokyo, Japan), followed by the construction of a three-dimensional maxillary model and fabrication of an extracted maxillary first premolar model. Four chronological models, immediately after tooth extraction, and after 1, 3, and 6 months, were fabricated by changing the CT values of the extracted area based on this model. A TAD was constructed in the mesial area of the upper first molar using SolidWorks software (SolidWorks, Tokyo, Japan). The upper first molar was constrained, and the upper canine was pulled in a distal direction towards the TAD at 1 N to analyze stress changes affecting the alveolar bone in the region of the extracted tooth.

Stress affecting the alveolar bone in the extracted region peaked immediately after tooth extraction, and gradually decreased with time. On the other hand, stress concentration was observed in the mesial alveolar crest of the extraction socket and the stress increased with ossification of the extraction socket. These results suggest that when using TAD it is more beneficial to apply tractive force soon after tooth extraction for distal tooth movement. (J Osaka Dent Univ 2015 ; 49(1) : 95–104)

Key words : Temporary anchorage device ; Three-dimensional finite element method ; Maxilla

INTRODUCTION

There are many different types of orthognathic surgery, such as sagittal split ramus osteotomy, for jaw deformities. Several surgeries are combined for difficult cases, such as simultaneous movement of the upper and lower jaws. In recent years, use of the TAD¹ and various methods of corticotomy have been considered as adjunctive surgical treatments^{2–4} in orthodontics for reduction of treatment time, simplification of the surgical procedures, and mitigation of surgical invasion. Orthodontic indications for the temporary screw type anchorage device became more common

with the introduction of coverage under the Japanese Social Insurance System for new medical technology in April 2014. This allows the use of the temporary screw type anchorage device for preoperative orthodontic treatment, opening the possibility for its more frequent application in the future. We constructed a three-dimensional model of the maxilla to evaluate the utility of the temporary screw type anchorage device for preoperative orthodontic treatment, and to investigate stress changes affecting the alveolar bone after extraction of first premolars using the three-dimensional finite element method.

MATERIALS AND METHODS

CT imaging

CT data of the maxilla of healthy adults was obtained using a CT system (Bright Speed, GE Medical System, New York, USA) in the Central Imaging Laboratory of Osaka Dental University Hospital at a tube voltage of 120 kV and a tube current of 120 mA with a slice thickness of 0.625 mm.

Extraction of image

We processed 110 CT images between the supraorbital margin and maxillary occlusal plane using Mechanical Finder version 6.2 in DICOM format (Fig. 1 A). Outlines of bone image areas were fabricated using the thresholding of each CT image (Fig. 1 B). For outline extraction, the external shape of the maxilla was obtained utilizing the higher CT value in bone than in its surrounding areas. Revisions in details were manually added based on CT images (Fig. 1 C).

Production of a three-dimensional maxillary model

The element size of the maxilla and a temporary screw type anchorage device was set at 0.5 mm using the oct-tree method.⁵ A mesh was generated by controlling the element size according to shape factors, and a three-dimensional maxillary model was fabricated including the infraorbital foramen on the top, maxillary occlusal plane on the bottom, and pterygoid base on the back (Fig. 2 A). A TAD model was then fabricated based on the shape of a screw of 1.0 mm in diameter and 5.0 mm in length using the three-dimensional computer-aided-design software SolidWorks (3D CAD) (Fig. 2 B). A fabricated TAD was constructed between the second premolar and the first molar of the maxillary three-dimensional model. A model of the maxilla following extraction of the bilateral maxillary first premolars was fabricated based on the above model (Fig. 2 C).

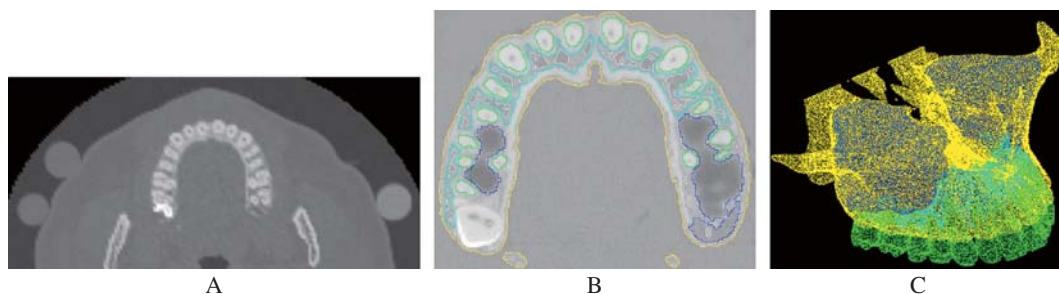


Fig. 1 Three-dimensional finite element models of (A) CT data of the maxilla of a healthy adult, (B) outlines of bone image areas, and (C) a mesh model of the maxilla.

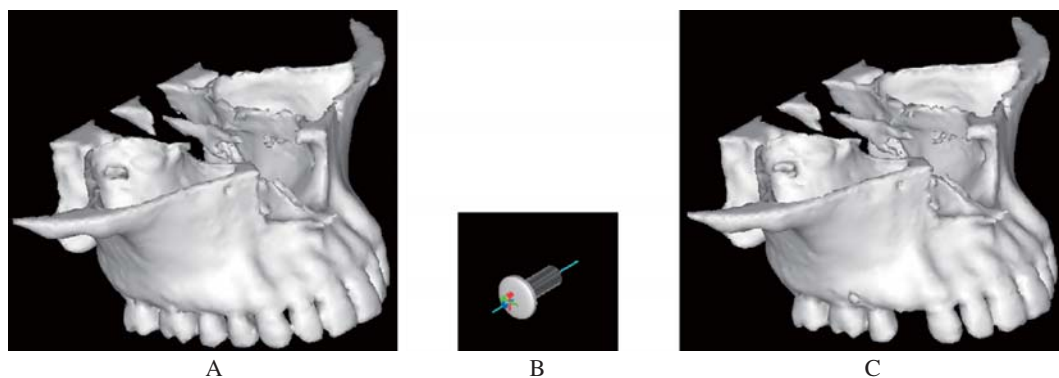


Fig. 2 Three-dimensional finite element models of (A) the maxilla, (B) an implant screw, and (C) the maxilla after extraction of the first premolar.

Construction material and substance properties

Construction materials of the model were cortical and cancellous bones, dental crown and root, and TAD. The bone, tooth, and TAD were defined by tetrahedral three-dimensional solid elements consisting of 4 nodal points and having three degrees of freedom with translation vectors in the X, Y and Z directions. The control model consisted of 142,634 elements and 31,261 tangent points.

Production of chronological models

CT was conducted 1 and 3 months after extraction of the upper first premolar (Fig. 3). A CT value of the extraction socket in the upper first premolar was imported from the data. CT values immediately after extraction, and 1, 3 and 6 months after extraction were changed using Solid Works, and four chronological models were fabricated. It was assumed that a blood clot would be present in the extraction socket immediately after tooth extraction, and that the extraction socket was completely healed at 6 months after extraction. A CT value of normal alveolar bone was used at 6 months. For CT values at 1 and 3 months postoperatively, average CT values of the extraction socket were used on the assumption that the CT value in the extraction socket was the same from the extraction socket base to the alveolar crest.

Determination of the physical properties

Young's module

Young's module (E) of each solid element was calculated from the CT value using formulas (1) and (2) below. There is a proportional relationship between the CT value (V_{CT}) and bone density (ρ), as shown in formula (1). In this formula, a and b were determined by simultaneous imaging of a bone mineral phantom [$Ca_{10}(PO_4)_6OH_2$]. The bone density of the extraction socket was calculated from a conversion formula (3) using a standard calibration curve since simultaneous radiography of a bone mineral phantom was not performed in a patient whose upper first premolar was extracted for orthodontic treatment. Young's modulus was calculated using formula (2) below based on the reports by Carter *et al.*⁶ and Akiyama *et al.*⁷ It was 6,000 for enamel, 1,400 for dentin, 1,100 for cortical bone, and 250 for cancellous bone. In this study, the strain rate (ϵ) was set at 0.01.

$$(1) \rho = a \cdot V_{CT} + b$$

$$(2) E = 3790 \epsilon^{0.06} \rho^3$$

$$(3) \rho = (V_{CT} + 1.4246) \times 0.001/1.0580$$

Poisson's ratio

Poisson's ratio was determined as 0.4 based on the report by Van Buskirk *et al.*⁸

Material properties of the TAD

The material properties of the TAD were that of pure titanium.

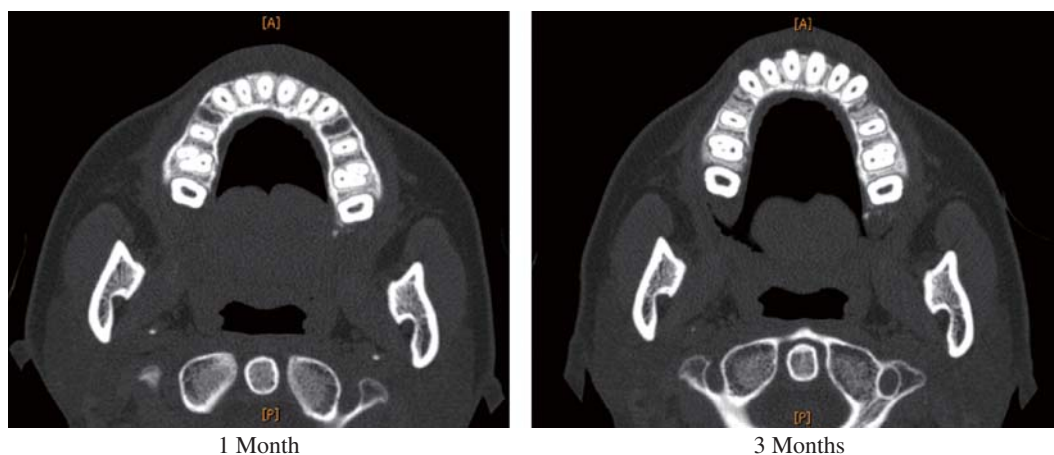


Fig. 3 CT data 1 and 3 months after extraction of the maxillary first premolar.

Loading and constraint

Constraint conditions

Constraint conditions included X on the horizontal axis, Y on the sagittal axis, and Z on the vertical axis. Nodal points at the top and bottom edges of the model were perfect constraints to reproduce continuity of the maxilla from the skull in the same manner as in the human body. The TAD and the bilateral maxillary first molars were also perfect constraints (Fig. 4).

Loading conditions

An orthodontic force of 1 N was applied from the upper canine in the TAD direction.

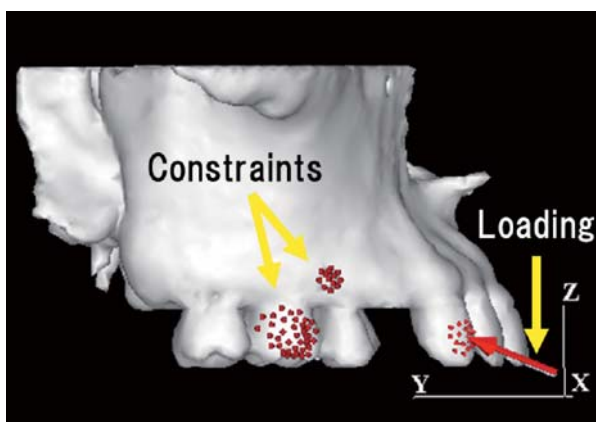


Fig. 4 Establishment of the loading direction and constraint points.

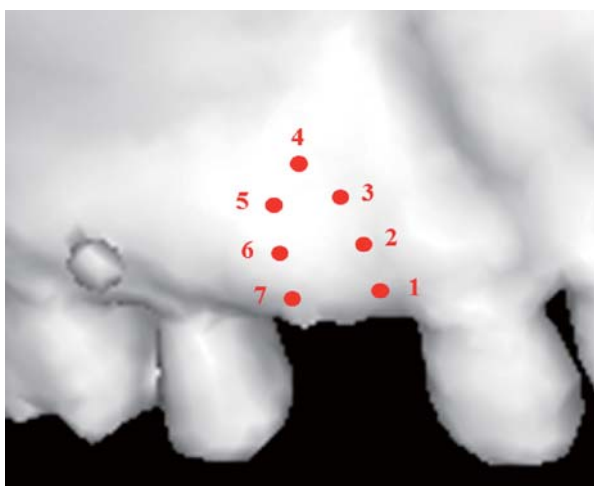


Fig. 5 Measurement points of equivalent stress on the cortical bone surface of the buccal alveolar bone (1–7).

Measurement points

Measurement points were the cortical bone surface of the buccal alveolar bone of the maxillary first premolar from 1 to 7 (Fig. 5), and points adjacent to the extraction socket in the alveolar central area from 8 to 14 (Fig. 6). Measurement points were located on the labial surface of the canine at (a) the center of the labial surface of the crown, (b) the center of the cervical area of the crown, (c) the center of the root labial surface, and (d) the apical area of the labial surface (Fig. 7). Measurement of displacement was performed on the incisal edge of the canine. The present study was ap-

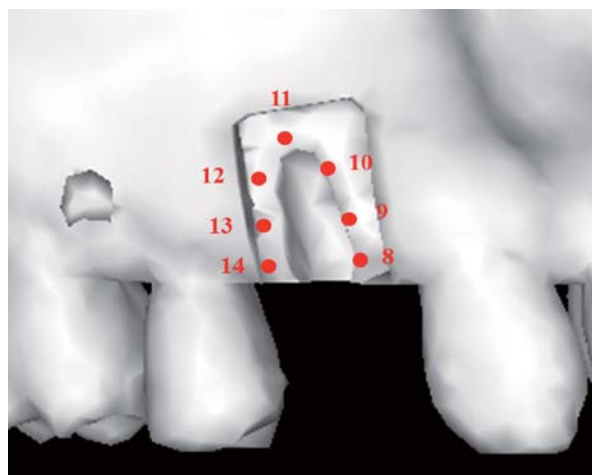


Fig. 6 Measurement points of the equivalent stress adjacent to the extraction socket in the central alveolar area (8–14).

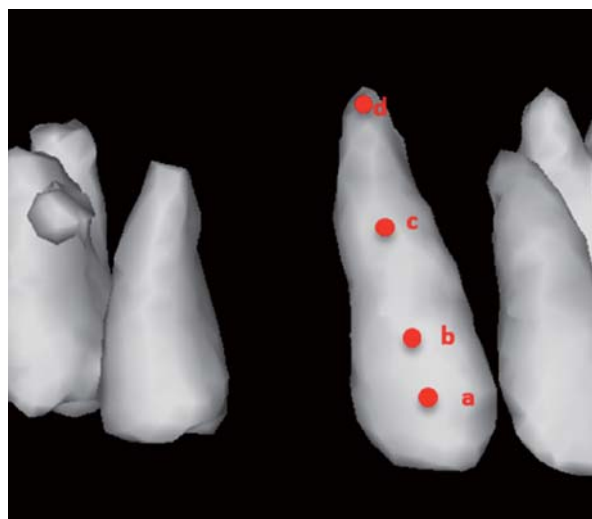


Fig. 7 Measurement points of the equivalent stress on the labial surface of the canine (a–d).

proved by the Ethics Committee of Osaka Dental University (Approval No. 110757).

RESULTS

Chronological stress distribution on the cortical bone of the buccal surface alveolar area

Stress distribution was observed from the canine area in the pulling direction (Fig. 8). Stress concentration was greatest in the mesial alveolar crest of the extraction area [measurement point 1] at 4.78×10^{-2} MPa immediately after extraction, and decreased over time to 4.73×10^{-2} MPa at 1 month, 4.50×10^{-2} MPa at 3 months, and reached its lowest level of 4.43×10^{-2} MPa at 6 months after extraction. It was also the greatest immediately after extraction, in points 2–6, decreased over time, and reached its lowest level at 6 months after extraction. According to the measurement points, the stress concentration was the greatest in the alveolar crest and gradually decreased towards the apical region. Stress decreased over time at all measurement points.

Comparison of measurement points between the

mesial and distal walls showed that stress was 1.8 times greater in the mesial wall than in the distal wall in the alveolar crest immediately after extraction. In the upper 1/3 of the dental root, stress was approximately 1.7 times greater in the mesial wall than in the distal wall, and in the lower 1/3 of the root it was approximately 1.2 times greater in the distal wall. Stress was approximately 2 times greater in the mesial wall than in the distal wall in the alveolar crest immediately after extraction. In the upper 1/3 of the dental root, stress was approximately 1.6 times greater in the mesial wall than in the distal wall, and in the lower 1/3 it was approximately 1.2 times greater.

Stress was approximately 2.1 times greater in the mesial wall than in the distal wall in the alveolar crest 3 months after extraction. In the upper 1/3 of the dental root, stress was approximately 1.5 times greater in the mesial wall than in the distal wall, and in the lower 1/3 of the root it was approximately 1.2 times greater in the distal wall. Stress was approximately 2.4 times greater in the mesial wall than in the distal wall in the alveolar crest at 6 months after extraction. In the up-

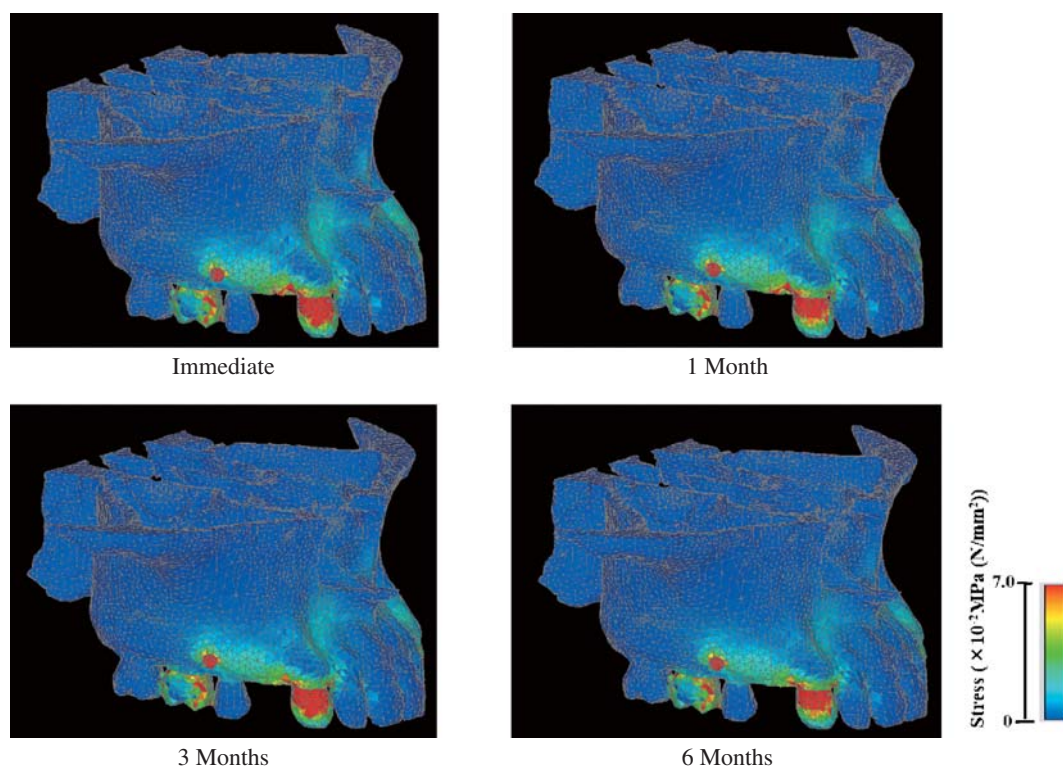


Fig. 8 Equivalent stress distribution on the cortical bone surface of the buccal alveolar bone.

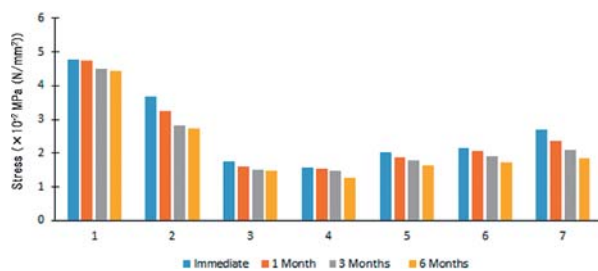


Fig. 9 Equivalent stress distribution on the cortical bone surface of the buccal alveolar bone.

Table 1 Equivalent stress distribution on the cortical bone surface of the buccal alveolar bone

Area	Immediate	1 Month	3 Months	6 Months
1	4.78	4.73	4.50	4.44
2	3.68	3.23	2.83	2.72
3	1.75	1.60	1.51	1.48
4	1.55	1.52	1.48	1.27
5	2.03	1.87	1.77	1.63
6	2.16	2.05	1.90	1.72
7	2.68	2.36	2.08	1.85

($\times 10^{-2}$ MPa(N/mm²))

per 1/3 of the dental root, stress was approximately 1.6 times greater in the mesial wall than in the distal wall, while in the lower 1/3 of the root it was approximately 1.1 times greater in the distal wall (Fig. 9, Table 1).

Chronological stress distribution in the cortical bone of the extraction socket

Stress concentration was observed in the mesial wall of the socket immediately after extraction. Stress was distributed over time in the distal wall and the socket 6 months after extraction (Fig. 10). Stress decreased in the measurement points from the alveolar crest to the apical area similar to the change over time of the stress on the cortical bone surface in the buccal alveolar area. However, stress was increased at 3 and 6 months after extraction compared with that immediately after extraction in points 8, 12, 13, and 14, and slightly decreased with time in points 9 and 10. A comparison of measurement points between the mesial and distal walls showed that stress was approximately

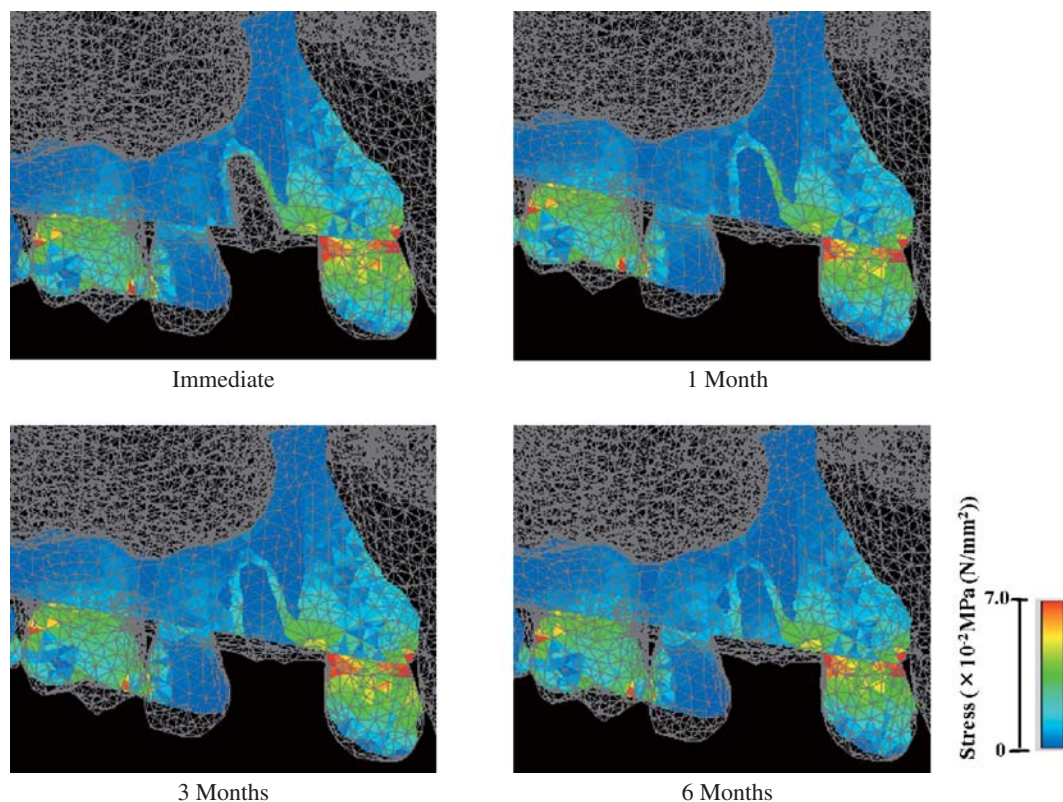


Fig. 10 Equivalent stress distribution adjacent to the extraction socket in the central alveolar area.

3.3 times greater in the mesial wall than in the distal wall immediately after extraction. In the upper and lower 1/3 of the dental root, stress was approximately 3 times greater in the mesial wall than in the distal wall, while in the lower 1/3 it was approximately 1.7 times greater in the mesial wall. Stress was approximately 3.4 times greater in the mesial wall than in the distal wall in the alveolar crest one month after extraction.

In the upper 1/3 of the root, stress was approxi-

Table 2 Equivalent stress distribution in the central alveolar area adjacent to the extraction socket

Area	Immediate	1 Month	3 Months	6 Months
8	2.97	2.96	3.36	3.40
9	1.75	1.78	1.56	1.57
10	1.14	1.08	1.02	1.01
11	0.95	0.93	0.92	0.88
12	0.66	0.63	0.89	1.03
13	0.59	0.61	1.04	1.10
14	0.89	0.85	1.60	1.78

($\times 10^{-2}$ MPa(N/mm²))

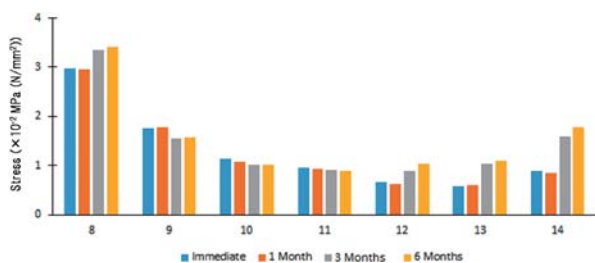


Fig. 11 Equivalent stress distribution adjacent to the extraction socket in the central alveolar area.

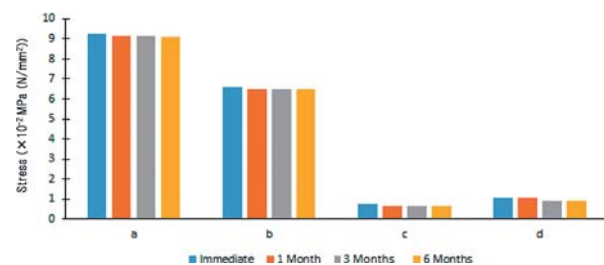


Fig. 13 Equivalent stress distribution on the labial surface of the canine.

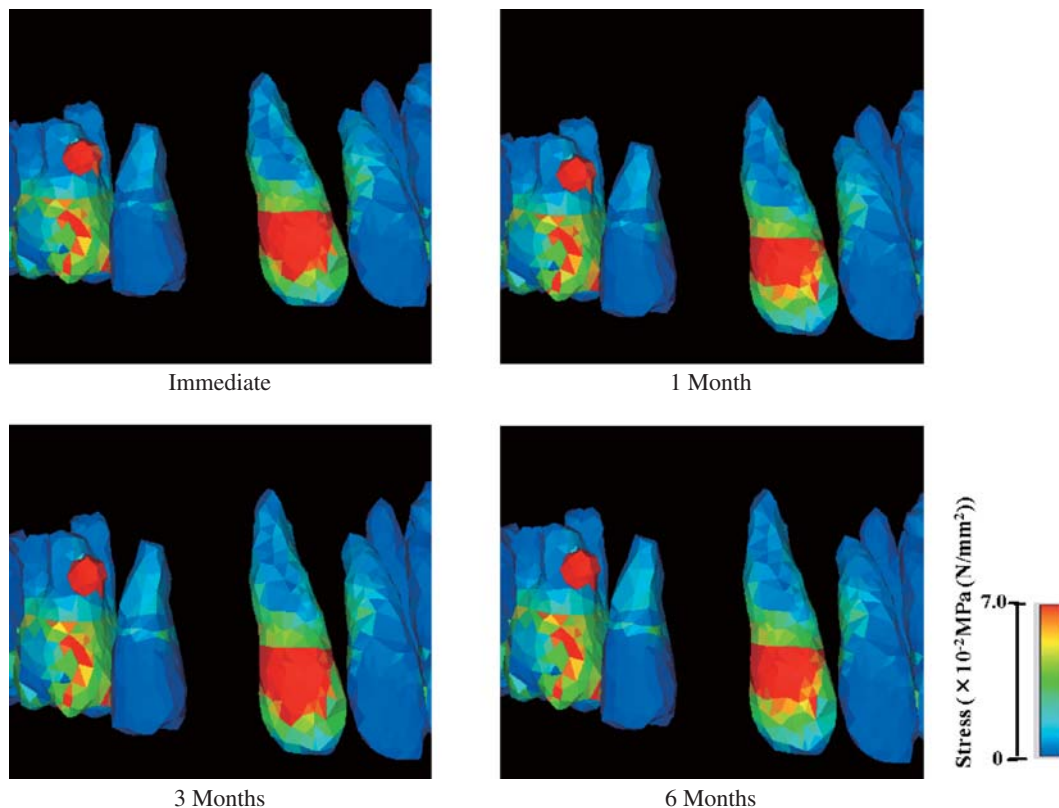
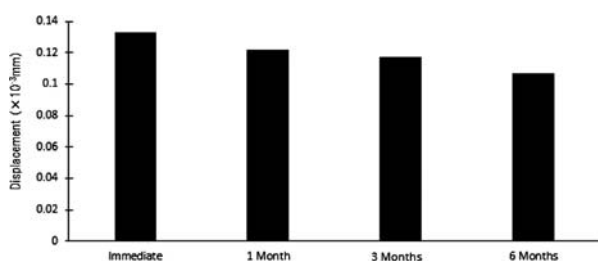


Fig. 12 Equivalent stress distribution on the labial surface of the canine.

Table 3 Equivalent stress distribution on the labial surface of the canine

Area	Immediate	1 Month	3 Months	6 Months
a	9.24	9.13	9.16	9.11
b	6.57	6.51	6.48	6.51
c	0.74	0.65	0.65	0.62
d	1.07	1.05	0.91	0.88

($\times 10^{-2}$ MPa(N/mm²))

**Fig. 14** Canine displacement.

mately 3 times greater in the mesial wall than in the distal wall, while in the lower 1/3 of the root it was approximately 1.7 times greater in the mesial wall. Stress was approximately 2 times greater in the mesial wall than in the distal wall in the alveolar crest 3 months after extraction. In the upper 1/3 of the dental root, stress was approximately 1.5 times greater in the mesial wall than in the distal wall, while in the lower 1/3 of the root it was approximately 1.2 times greater. Stress was approximately 2 times greater in the mesial wall than in the distal wall in the alveolar crest 6 months after extraction. In the upper 1/3 of the dental root, stress was approximately 1.4 times greater in the mesial wall than in the distal wall, while in the lower 1/3 of the dental root, stress in the mesial and distal walls were the same (Fig. 11, Table 2).

Chronological stress distribution in the canine region

High stress concentration was observed between the labial surface of the canine, which is a loading base point, and the cervical area in the canine. Stress was lower in the root than in the crown (Fig. 12). There was no chronological change in stress among the measurement points (Fig. 13, Table 3).

Table 4 Canine displacement

	Immediate	1 Month	3 Months	6 Months
Displacement	0.13	0.12	0.12	0.11

($\times 10^{-3}$ mm)

Tooth displacement at the canine incisal edge

The amount of tooth displacement peaked immediately after extraction at 0.13310^{-3} mm, gradually decreased between 1 and 6 months, and reached a minimum at 6 months of 0.10710^{-3} mm (Fig. 14, Table 4).

DISCUSSION

An increasing number of adults have been seeking surgical orthodontic treatment. Problems of orthodontic treatment in adult patients include periodontitis, tooth loss and restorations. Anchorage problems during tooth movement are often encountered in adult orthodontic treatment. Since Creekmore and Eklund⁹ reported an overbite case treated by upper anterior teeth intrusion using Vitallium and bone screws in 1983, various shapes of TAD¹⁰ have been suggested, including the dental implant type, the mini plate type, and the mini screw type. They allow tooth intrusion and posterior molar movement, which is difficult with conventional orthodontic treatment. The mini screw-type TAD, in particular, involves an easy implantation procedure, has low invasiveness, and poses a minimal burden to patients. The screw-type TAD was approved as an orthodontic device by the Pharmaceutical Affairs Act in Japan in August 2012, which allowed the introduction of TAD into orthodontic treatment.

TAD became more common in preoperative orthodontic treatment with the introduction of coverage under the Japanese Social Insurance System for new medical technology in April 2014. TAD application in preoperative orthodontic treatment allows the avoidance of a surgical procedure, shortening of the treatment period, and simplification of the surgical procedure. It is thought that the frequency of TAD use will increase in the future. In order to investigate the effectiveness of preoperatively applied TAD, we construc-

ted a three-dimensional finite element model of the maxilla and analyzed the stresses on the alveolar bone in the extraction area during upper canine traction when the upper first premolar was extracted.

Stress change in the cortical bone of the buccal alveolar bone

Although stress in the cortical bone of the buccal alveolar bone peaked immediately after extraction at each measurement point, and decreased over time, the greatest stress was observed in the mesial alveolar crest at each observation point. Togo *et al.*¹¹ performed distal en masse movement of the maxillary anterior teeth, followed by analysis using the three-dimensional finite element method, and reported that it showed greatest stress concentration in the distal cervix of the maxillary anterior teeth. We also found the greatest stress concentration in the distal cervix of the canines. High stress was observed in the mesial area of the alveolar crest, in the upper 1/3 of the dental root, and in the distal area of the lower 1/3 of the apical region. This is considered to have been due to the fact that a load was placed on the buccal surface of the maxillary canine, which was a loading base point in the TAD direction; therefore, higher stress was observed in the distal area than in the mesial area of the apical 1/3 of the buccal alveolar region in the same direction as the loading vector.

Stress change in the cortical bone of the central extraction socket

Although the highest stress was observed in the mesial alveolar crest in the cortical bone of the central extraction socket, stress was generally low compared with that on the buccal cortical bone. The change in stress over time in the mesiodistal alveolar crest and distal wall increased, while the stress change in the buccal cortical bone decreased. However, the stress decreased in the upper 1/3 and apical 1/3 of the mesial root, the same as in the buccal cortical bone. The opposite changes in the buccal cortical bone and extraction socket are considered to have been due to the fact that stress spread into the extraction socket and reached the distal wall with ossification of the extraction socket.

Stress and amount of displacement of the canine

Stress on the canine was the greatest at the loading point and lowest in the apical 1/3 region. Since the center of the crown was simply pulled, the apical 1/3 became the center of rotation. There was little change in stress over time. Togo *et al.*¹¹ reported that the amount of displacement was 0.10910^{-3} mm when the canine was distally pulled using a TAD placed on the maxillary first molar and apical 2 mm of the second premolar. Our results were approximately the same as those in the report of Togo *et al.*¹¹ at 6 months. However, the amount of displacement was the greatest immediately after extraction and decreased over time. It seems that the amount of displacement decreased as the stress was distributed in the extraction socket by ossification.

In order to investigate the effectiveness of the TAD in tooth movement, we measured the stress distribution in the extraction socket and alveolar cortical bone over time. Stress was the greatest in the mesial area of the socket immediately after extraction. Although an increase in stress over time was observed in the cortical bone of the extraction wall, this is because stress concentration was dispersed due to ossification of the extraction socket. The amount of tooth displacement was the greatest immediately after extraction. These results suggest that early traction before callus formation in the extraction socket followed by distal traction of the upper anterior teeth is effective when the maxillary premolar has been extracted.

REFERENCES

1. Motoyoshi M. Clinical application of mini-implants for orthodontic. *Nihon Univ Dent J* 2011; **85**: 111–115. (Japanese)
2. Motohashi T, Nakajima M, Kakudo K. Three-dimensional finite element stress analysis on compression osteogenesis. *Jpn J Jaw Deform* 2007; **17**: 1–8. (Japanese)
3. Nakajima M, Kakudo K, Onishi Y, Morishita H, Tsunokuma M, Kim H, Kawamoto T, Yunoki H. Compressive osteogenesis for maxillary protrusion. *Jpn J Jaw Deform* 2003; **13**: 127–133. (Japanese)
4. Ozaki K, Nakajima M, Kakudo K. Biomechanical analysis of corticotomy. *J Osaka Dent Univ* 2013; **47**: 171–178.
5. Chen HH, Huang TS. A survey of construction and manipulation of octrees. *Comput Graphics Image Processing* 1988; **43**: 409–431.
6. Carter DR, Hayes WC. The compressive behavior of bone as a two-phase porous structure. *J Bone Joint Surg* 1977; **59A**: 954–962.
7. Akiyama C, Hara S, Kamezawa H, Yokozuka S. Stress analy-

- sis of tooth and supporting tissue using the finite element method. *Shigaku* 1999 ; **86** : 783–793. (Japanese)
8. Van Buskirk WC, Ashman B. The elastic moduli of bone. *Trans Am Soc Mech Eng* 1981 ; **45** : 131–143.
9. Creekmore TD, Eklund MK. The possibility of skeletal anchorage. *J Clin Orthod* 1983 ; **17** : 266–269.
10. Sugawara J, Kanzaki R, Takahashi I, Nagasaka H, Nanda R. Distal movement of maxillary molars in nongrowing patients with the skeletal anchorage system. *Am J Orthod Dentofacial Orthop* 2006 ; **129** : 723–733. (Japanese)
11. Togo S, Katada H, Sueishi K. Biomechanical evaluation in distal en masse movement of maxillary dentition by implant anchorage –three-dimensional finite element stress analysis–. *The Shikwa Gakuho* 2010 ; **110** : 319–330. (Japanese)